

See discussions, stats, and author profiles for this publication at: <https://www.researchgate.net/publication/235879215>

# Performance of Density Functional Methods. Some Difficult Cases for Small Systems Containing Cu, Ag, or Au

ARTICLE *in* THE JOURNAL OF PHYSICAL CHEMISTRY A · MARCH 2013

Impact Factor: 2.69 · DOI: 10.1021/jp3115572 · Source: PubMed

---

CITATIONS

4

---

READS

46

3 AUTHORS, INCLUDING:



[Anibal Sierraalta](#)

Venezuelan Institute for Scientific Research

94 PUBLICATIONS 794 CITATIONS

SEE PROFILE



[Rafael Añez](#)

Venezuelan Institute for Scientific Research

43 PUBLICATIONS 187 CITATIONS

SEE PROFILE

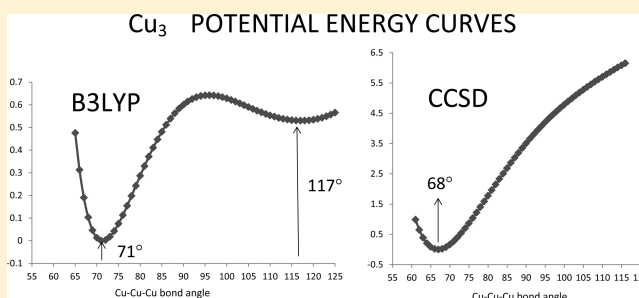
# Performance of Density Functional Methods. Some Difficult Cases for Small Systems Containing Cu, Ag, or Au

Anibal Sierraalta,\* Rafael Añez, and Paola Alejos

Laboratorio de Química Computacional, Centro de Química, Instituto Venezolano de Investigaciones Científicas, Apartado 21827, Caracas 1020-A, Venezuela

## Supporting Information

**ABSTRACT:** Twenty-six density functional theory (DFT) methods were tested in conjunction with three different effective core potentials (ECPs) and their corresponding valence basis sets, for studying the behavior of DFT methods in small systems containing Cu, Ag, or Au where it is well-known that some functionals fail. The DFT results were compared with those obtained with post Hartree–Fock methods: second-order many-body perturbation theory (MP2), coupled cluster singles-doubles (CCSD), and coupled cluster singles-doubles with perturbative triples, CCSD(T). Calculations were carried for  $M_3$  ( $M = \text{Cu, Ag, Au}$ );  $M_4^-$  ( $M = \text{Cu, Ag}$ ) and  $[\text{H}_2\text{O}-\text{Cu}]^{+2}$ . The comparison of the DFT calculated values with the Post Hartree–Fock values showed that, in general, all generalized gradient approximation (GGA) type functionals fail to describe these systems. The hybrid GGA functionals (H-GGA) showed a better behavior; however, when the Lee–Yang–Parr (LYP) exchange–correlation functional was used, wrong results were obtained. The results with the hybrid meta (HM-GGA) functionals, as in the case of H-GGAs, showed that, to obtain similar results to MP2 or CCSD(T), it is necessary to have a high Hartree–Fock exchange percentage. Spurious results obtained with the H-GGA or HM-GGA methods can be eliminated increasing the Hartree–Fock exchange percentage in the H-GGA or HM-GGA type functionals. Among the different functionals tested, the BB1K and MPWB1K functionals showed the best agreement with the MP2 and CCSD(T) results.



## INTRODUCTION

Presently, common computational quantum chemistry applications include calculations of minimum energy structures, activation energies, thermodynamic properties, vibrational frequencies, atomic charges, and so forth. These types of calculations aid scientists in their interpretation of experimental results, and therefore, it is very important to know the limitations of the quantum chemistry methods to avoid false conclusions extracted from the calculations. Nowadays, quantum chemical calculations performed using density functional theory (DFT) have become a very common application.<sup>1,2</sup> However, since the exact exchange–correlation functional is not known, only approximate functionals can be used,<sup>2</sup> which introduces limitations and errors in the calculation results. There are a large number of papers devoted to validating the density functionals.<sup>1–3</sup> Experimental or high level wave function theory data are used for the functional validation, and in general, but not always,<sup>4</sup> the mean unsigned error (MUE) is reported. The MUE value gives an idea of the precision of the density functionals; for example, Barden et al.<sup>5</sup> analyzed the behavior of some density functionals in the calculation of nine homonuclear 3d dimers. The authors found that, for B3LYP, the bond distance MUE value was 0.053 Å; therefore, one cannot expect values for 3d bond distances better than  $\pm 0.05$  Å.

Recently, some authors have reported limitations, failures, or wrong answers in the calculations with some density functionals. Ramírez-Solís<sup>6</sup> in a systematic study about the performance of local density approximation (LDA), generalized gradient approximation (GGA), and nonlocal hybrid and meta type functionals on transition metal molecules found that the hybrid functionals were able to correctly reproduce the ordering for the lowest five electronic states of  $\text{CuCl}_2$  and  $\text{AgCl}_2$ . However, they are incapable of reproducing a potential curve for the lowest triplet state of  $\text{AgI}$ . Sodupe and co-workers<sup>9</sup> have shown that the popular B3LYP functional along with G96LYP, BLYP, and MPW1PW91 are unable to reproduce the relative energies of the ground and low-lying electronic states of the  $[\text{H}_2\text{O}-\text{Cu}]^{+2}$  complex. B3LYP wrongly predicts that the  $^2A'$  state ( $C_s$  symmetry) is the ground state and the  $^2A_1$  state ( $C_{2v}$  symmetry) the second low-lying state, in complete disagreement with CCSD(T) results where the  $^2A'$  state does not exist and the ground state corresponds to the  $^2A_1$  state. Li et al.,<sup>7</sup> in a theoretical study on  $\text{Au}_n^+$  ( $n = 4-6$ ) clusters, found that the DFT relative energy between  $C_{2v}$  and quasi- $D_{3h}$  structure for  $\text{Au}_6^+$  clusters was positive or negative

Received: November 23, 2012

Revised: March 2, 2013

Published: March 6, 2013

Table 1. Summary of the Density Functionals Employed in This Work<sup>a</sup>

type	HF exchange weight factor	functional	exchange functional	correlation functional
GGA	0	BLYP <sup>22,23</sup>	Becke88	Lee–Yang–Parr
GGA	0	OLYP <sup>22,24</sup>	OptX	Lee–Yang–Parr
GGA	0	MPWLYP <sup>23,25,26</sup>	modified Perdew–Wang91	Lee–Yang–Parr
GGA	0	MPWP86 <sup>25,27</sup>	modified Perdew–Wang91	Perdew86
GGA	0	BP86 <sup>27,23</sup>	Becke88	Perdew86
GGA	0	MPWPW91 <sup>25,26</sup>	modified Perdew–Wang91	Perdew–Wang91
GGA	0	BPW91 <sup>27,23</sup>	Becke88	Perdew–Wang91
GGA	0	MPWPBE <sup>25,28</sup>	modified Perdew–Wang91	Perdew–Burke–Ernzerhof
GGA	0	PBEPBE <sup>28</sup>	Perdew–Burke–Ernzerhof	Perdew–Burke–Ernzerhof
H-GGA	0.1161	O3LYP <sup>23,24</sup>	OptX	Lee–Yang–Parr
H-GGA	0.200	B3LYP <sup>23,24,30</sup>	Becke88	Lee–Yang–Parr
H-GGA	0.200	B3PW91 <sup>26,23,31</sup>	Becke88	Perdew–Wang91
H-GGA	0.200	B3P86 <sup>27,22,29</sup>	Becke88	Perdew86
H-GGA	0.210	B97-1 <sup>32</sup>	B97-1	B97-1
H-GGA	0.218	X3LYP <sup>23,23,33</sup>	Becke88 + Perdew–Wang91	Lee–Yang–Parr
H-GGA	0.218	MPW3LYP <sup>23,25,26</sup>	modified Perdew–Wang91	Lee–Yang–Parr
H-GGA	0.250	PBE1PBE <sup>28</sup>	Perdew–Burke–Ernzerhof	Perdew–Burke–Ernzerhof
H-GGA	0.428	MPW1K <sup>25,26,34,35</sup>	modified Perdew–Wang91	Perdew–Wang91
H-GGA	0.500	BH&HLYP <sup>22,31</sup>	Becke88	Lee–Yang–Parr
HM-GGA	0.150	MPW1KCIS <sup>25,27,36,37</sup>	modified Perdew–Wang91	Krieger–Chen–Iafrate–Savin
HM-GGA	0.220	PBE1KCIS <sup>28,36,38</sup>	Perdew–Burke–Ernzerhof	Krieger–Chen–Iafrate–Savin
HM-GGA	0.280	B1B95 <sup>22,31</sup>	Becke88	Becke95
HM-GGA	0.310	MPW1B95 <sup>25,26,33,33</sup>	modified Perdew–Wang91	Becke95
HM-GGA	0.420	BB1K <sup>22,31,39</sup>	Becke88	Becke95
HM-GGA	0.420	BMK <sup>40</sup>	BMK	BMK
HM-GGA	0.440	MPWB1K <sup>25,26,31,41</sup>	modified Perdew–Wang91	Becke95

<sup>a</sup>See ref 1 for a complete review on DFT functionals.

depending on the density functional. On the other hand, with *ab initio* correlated methods, such as second-order many-body perturbation theory (MP2), coupled cluster singles-doubles (CCSD), or coupled cluster singles-doubles with perturbative triples (CCD(T)), the relative energy was always negative. Schwerdtfeger and co-workers<sup>10</sup> studied the interaction of CO with anionic, neutral, and cationic Au<sub>2</sub> molecules. From the analysis of their results, the authors found that the different density functionals studied by them were not able to correctly describe the interaction between CO and gold. Unfortunately, Schwerdtfeger et al.<sup>10</sup> only studied two GGA type functionals and one hybrid type functional, namely, B3LYP. In regard to Sodupe and co-workers,<sup>9</sup> they did not include hybrid-meta type functionals in their study, and Li et al.<sup>7</sup> did not analyze the influence of the Hartree–Fock exchange of the hybrid functionals on their results.

Schaefer III et al.<sup>8</sup> studying Ag<sub>3</sub> clusters and using 23 density functional methods found that the density functionals with the LYP and B97 correlation functionals predict only one minimum with an obtuse apex angle of ~140° for the neutral silver trimer while CCSD(T) predicts one minimum with an apex angle of ~69°; moreover, other group of functionals predicted wrongly the existence of two minima. This last result along with the previous ones seem to point out that the problem found for Ag<sub>3</sub> clusters could be more general and would be present in other small metallic clusters as well as in complexes such as [H<sub>2</sub>O–Cu]<sup>+2</sup>.

According to the former discussion, it seems that the limitations, weakness, or strength of the density functionals proposed in the literature are not totally clear. Despite theoretical studies performed, some important questions remain unanswered: Which one is the most reliable functional

at the moment for calculation of small metallic clusters? Is there some kind of diagnostic that can be applied to know how reliable the results are? In this work we study the following systems: M<sub>3</sub>, M = Cu, Ag, Au; M<sub>4</sub><sup>+</sup>, M = Cu, Ag and [H<sub>2</sub>O–Cu]<sup>+2</sup> where it is known that the many density functionals fail. The aim of the present work is to aid in the understanding of the failures and limitations and help to improve the behavior proposed as functional in the literature.

## METHODOLOGY

All geometry optimizations, energy, and frequency calculations were performed with the Gaussian-03 program.<sup>11</sup> A total of 26 density functionals were tested. The functionals were chosen as follows: 9 GGA, see Table 1. These types of functionals include in the exchange-correlation expression not only the density,  $\rho$  as in the local density approximation methods, but also the gradient of the density. Ten H-GGA functionals which employ the generalized gradient approximation adding to the exchange-correlation part of the GGA, the Hartree–Fock exchange weighted by a factor, which is lower than 1. Seven HM-GGA functionals which include higher order density gradients than the corresponding to the GGA and the kinetic energy density; these expressions are not included in the standard GGA methods. As in the case of the H-GGA, the HM-GGA also includes the Hartree–Fock exchange.<sup>1</sup> Table 1 presents a summary of the density functionals employed in this work. Post-HF calculations were performed using the CCSD,<sup>12</sup> CCSD(T),<sup>13</sup> and the Møller–Plesset method truncated at second order, MP2.

Three effective core potentials (ECPs) along with their valence basis sets were employed in this work. All ECPs include explicitly the 19 valence electrons  $ns^2np^6nd^{10}(n+1)s^1$ . The

LanL2DZ or Los Alamos ECP<sup>14</sup> has a double- $\zeta$  quality basis sets; [5s,6p,4d/3s,3p,2d] for Cu and Ag, and [5s,6p,3d/3s,3p,2d] for Au. The medium size CEP-121 or compact effective potentials<sup>15</sup> has a triple-split or triple- $\zeta$  quality basis sets; [8s,8p,6d/4s,4p,3d] for Cu, [8s,8p,5d/4s,4p,3d] for Ag and [7s,7p,5d/4s,4p,3d] for Au. The SDD ECP or the energy-consistent pseudopotentials of the Stuttgart/Cologne Group known as Stuttgart–Dresden<sup>16</sup> has the largest basis sets [8s,7p,6d/6s,5p,3d] for Cu, Ag, and Au. To avoid numerical problems in the calculation of the exchange–correlation energies, all calculations were performed with the grid ultrafine. All optimization were performed with a tight criterion. The root-mean-square (RMS) force is equal to  $1 \times 10^{-5}$ , and the RMS of the displacement is equal to  $4 \times 10^{-5}$ . For the optimization processes, two techniques were employed: (a) relaxed potential energy surface scans with regular intervals sampling of the angles and relaxing the bond distances and, (b) global optimization from a given starting structure. The spin–orbit coupling and the BSSE corrections were not included in the calculations.

## RESULTS AND DISCUSSION

**A. Diatomic Molecules: Cu<sub>2</sub>, Ag<sub>2</sub>, and Au<sub>2</sub>.** To have a look at the goodness of the density functionals to reproduce experimental data, we performed DFT calculations for Cu<sub>2</sub>, Ag<sub>2</sub>, and Au<sub>2</sub> using the 26 functionals reported in Table 1 and the three sets of ECP/valence basis sets. We calculated the MUEs using the experimental data reported on ref 17. The calculated MUE values of the bond lengths for GGA methods were 0.07, 0.07, and 0.06 Å for LanL2DZ, CEP-121, and SDD, respectively. The average mean unsigned errors (AMUEs), which is the average of the MUEs with the LanL2DZ, CEP-121, and SDD ECP/valence basis sets, was 0.07 Å. This last value compare well with the reported value by Truhlar et al.<sup>18</sup> (0.09 Å) in their study on density functionals where the authors analyzed the bond lengths as well as atomization energies of eight transition metal dimers, including Cu<sub>2</sub> and Ag<sub>2</sub>. For the H-GGA methods, our MUE values were 0.07, 0.07, and 0.07 Å for LanL2DZ, CEP-121, and SDD, respectively, and the AMUE 0.07 Å. For HM-GGA methods, the calculated MUE values were 0.07, 0.07, and 0.06 Å for LanL2DZ, CEP-121, and SDD, respectively, and the AMUE 0.07 Å. All our AMUE values are lower than the reported for the set of eight metallic dimers<sup>18</sup> (0.09 Å for GGA, 0.18 Å for H-GGA, and 0.15 Å for HM-GGA) but higher than the corresponding to the subset composed by Ag<sub>2</sub>, AgCu, Cu<sub>2</sub>, and Zr<sub>2</sub> (0.05 Å for GGA, 0.05 Å for H-GGA, and 0.04 Å for HM-GGA).<sup>18</sup> The reason for this is that the set of eight metallic dimers includes the Cr<sub>2</sub> molecule where, according to Truhlar et al.,<sup>18</sup> the DFT methods fail to reproduce the experimental Cr<sub>2</sub> bond distance. On the other hand, our set includes the Au<sub>2</sub> molecule where it is well-known<sup>10</sup> that the DFT methods do not reproduce the bond length and the dissociation energy; therefore, our MUEs values are larger than the corresponding to the subset of Ag<sub>2</sub>, AgCu, Cu<sub>2</sub>, and Zr<sub>2</sub>.

**B. Neutral Trimer Structures: Cu<sub>3</sub>, Ag<sub>3</sub>, and Au<sub>3</sub>.** Schaefer III et al.<sup>8</sup> reported that, for neutral and ionic Ag<sub>3</sub> clusters, the molecular geometry are highly depend on the correlation functional employed in the calculation. The authors studied 23 DFT methods and found a better performance when the uniform electron gas limit is incorporated into the correlation functional, whereas in those methods with LYP type functionals or variations of the B97 the performance was

worse. In this section, we study the Cu<sub>3</sub>, Ag<sub>3</sub>, and Au<sub>3</sub> clusters with 26 different density functionals and with the ab initio post-Hartree–Fock methods CCSD, CCSD(T), and MP2. According to Table 2 at CCSD, CCSD(T), and MP2/SDD levels, the

**Table 2. Distances (in Å) and Bond Angles (in Degrees) for Cu<sub>3</sub>(C<sub>2v</sub>) Clusters. <sup>2</sup>B<sub>2</sub> State Using Some GGA Type Functional<sup>a</sup>**

functional	R (Å)	angle (deg)	R (Å)	angle (deg)
BLYP	2.319	71.96	2.310	122.98
	2.338	68.62	2.329	125.35
	<b>2.308</b>	<b>69.85</b>	<b>2.304</b>	<b>128.70</b>
OLYP	2.367	72.39	2.370	121.06
	2.357	68.95	2.364	116.50
	<b>2.339</b>	<b>70.00</b>	<b>2.351</b>	<b>124.27</b>
MPWLYP	2.317	71.87	2.307	122.50
	2.335	68.53	2.326	124.54
	<b>2.305</b>	<b>69.67</b>	<b>2.300</b>	<b>128.43</b>
MPWP86	2.303	68.94	2.275	117.04
	2.310	67.12		
	<b>2.286</b>	<b>67.59</b>		
BP86	2.306	68.98	2.299	114.26
	2.313	67.17		
	<b>2.289</b>	<b>67.68</b>	<b>2.279</b>	<b>118.43</b>
MPWPW91	2.312	68.96		
	2.316	67.11		
	<b>2.293</b>	<b>67.58</b>		
BPW91	2.315	69.00		
	2.319	67.16		
	<b>2.296</b>	<b>67.66</b>		
MPWPBE	2.312	68.83		
	2.315	67.02		
	<b>2.292</b>	<b>67.48</b>		
PBEPBE	2.317	68.75		
	2.319	66.96		
	<b>2.297</b>	<b>67.45</b>		

<sup>a</sup>LanL2DZ plain. CEP-121 italic. SDD bold. MP2: LanL2DZ R = 2.402, angle = 69.34; CEP-121 R = 2.290, angle = 66.69; SDD R = **2.297**, angle = **66.59**. CCSD: LanL2DZ R = 2.432, angle = 70.75; CEP-121 R = 2.336, angle = 68.56; SDD R = **2.334**, angle = **68.40**. CCSD(T): LanL2DZ R = 2.420, angle = 69.54; CEP-121 R = 2.322, angle = 67.09; SDD R = **2.323**, angle = **66.86**.

Cu<sub>3</sub> cluster only has one minimum energy structure with an acute bond angle of  $\sim 67^\circ$ . At the DFT level with a SDD ECP/valence basis set, within GGA approximation, the number of minimum energy structures depends on the correlation functional; that is, for LYP (see Figure 1) and P86 correlation functionals, there are two structures, while for PW91 and PBE there is only one. These results are similar to those reported by Schaefer III et al.<sup>8</sup> Table 3 shows that for Ag<sub>3</sub> cluster at CCSD, CCSD(T), and MP2, there is only one stationary point that corresponds to the geometry with a bond angle of  $\sim 68^\circ$ . Even though for BLYP, OLYP, and MPWLYP only one structure was found, the angle is above  $139^\circ$ , and therefore these results are in disagreement with the ab initio post-Hartree–Fock results. The others GGA functionals predict two minimum energy structures, one with an acute Ag–Ag–Ag bond angle ( $\sim 70^\circ$ ) and other with an obtuse bond angle ( $\sim 135^\circ$ ), again in conflict with CCSD, CCSD(T), and MP2 results. In the case of Au<sub>3</sub> clusters, the CCSD/SDD calculations show that there are two stationary points, one at  $r = 2.700$  Å and  $\theta = 65.7^\circ$ , and the



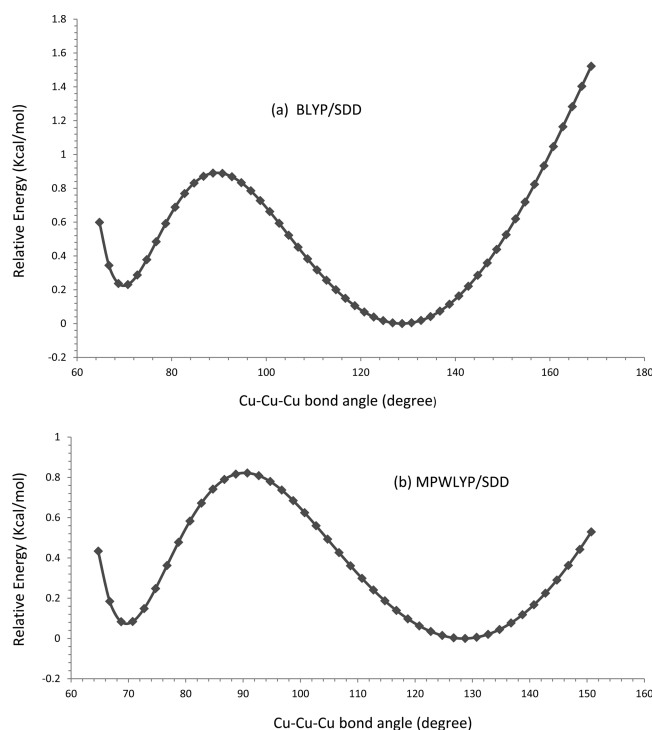


**Figure 1.** Potential energy curve for the  $\text{Cu}_3$  as a function of the Cu–Cu–Cu bond angle. (a) BLYP/SDD, (b) MPWLYP/SDD.

other one at  $r = 2.625 \text{ \AA}$  and  $\theta = 122.4^\circ$ . Surprisingly, all of the GGA functionals tested with CEP-121 predict two minima, one at  $\sim 68^\circ$  and the other at  $\sim 136^\circ$  in agreement with the CCSD results. On the other hand when LanL2DZ is used, only the structure with the obtuse bond angle ( $\sim 147^\circ$ ) is obtained with BLYP, OLY, and MPWLYP functionals. The other functionals with LanL2DZ predict qualitatively the two minimum energy structures. With SDD, all GGA functionals predict two minima in agreement with the CCSD/SDD result except the OLYP functional where only the structure with the obtuse bond angle was obtained. To know if the trend found with the GGA type functionals remains when increasing the quality of the valence basis set, calculations with def2-QZVP ECP basis set<sup>19,20</sup> and four functionals: BLYP, MPWLYP, MPWPW91 and PBEPBE, were performed. The results show that for  $\text{Cu}_3$ , similarly to the results obtained with LANL2DZ, CEP-121, and SDD (see Table 2), the BLYP and MPWLYP functionals predict two minima at  $\sim 69^\circ$  and  $\sim 126^\circ$ , while the MPWPW91 and PBEPBE predict only one minimum near to  $67^\circ$ . For  $\text{Ag}_3$ , the BLYP and MPWLYP functionals predict one minimum near to  $144^\circ$ , while with the MPWPW91 and PBEPBE functionals two minima at  $\sim 69^\circ$  and  $\sim 133^\circ$  were obtained. Regarding the H-GGA type functionals, calculations with a new split LanL2DZ and CEP-121 valence basis sets were performed. The new valence basis sets corresponding to LanL2DZ ECP for Cu and Ag (5s, 5p, 3d) have two s, two p, and one d extra functions. These valence basis sets are known in the literature as LanL2TZ.<sup>20</sup> For CEP-121 ECP, the original (4s, 4p, 3d) valence basis set was extended to (6s, 6p, 4d). Calculation for  $\text{Cu}_3$  and  $\text{Ag}_3$  using the X3LYP functional with these new extended valence basis sets only shows a change of bond distance and bond angle values but not in the number of minimum energy structures. The number of minima obtained with def2-QZVP ECP/basis set, LanL2TZ, and the extended CEP-121 is qualitatively similar to those obtained with the

**Table 3.** Distances (in  $\text{\AA}$ ) and Bond Angles (in Degrees) for  $\text{Ag}_3(\text{C}_{2v})$  Clusters.  $^2\text{B}_2$  State Using Some GGA Type Functional<sup>a</sup>

functional	R ( $\text{\AA}$ )	angle (deg)	R ( $\text{\AA}$ )	angle (deg)
BLYP			2.697	144.86
			2.692	140.14
			<b>2.676</b>	<b>157.19</b>
OLYP			2.743	151.75
			2.723	144.25
			<b>2.709</b>	<b>180.0</b>
MPWLYP			2.693	144.36
			2.688	139.30
			<b>2.672</b>	<b>159.87</b>
MPWP86	2.653	71.40	2.651	135.89
	2.649	69.21	2.644	131.06
	<b>2.635</b>	<b>70.17</b>	<b>2.629</b>	<b>142.85</b>
BP86	2.655	71.73	2.653	136.34
	2.651	69.42	2.648	131.93
	<b>2.637</b>	<b>70.48</b>	<b>2.632</b>	<b>141.99</b>
MPWPW91	2.661	72.08	2.661	135.03
	2.655	69.54	2.653	131.04
	<b>2.672</b>	<b>70.54</b>	<b>2.638</b>	<b>142.80</b>
BPW91	2.663	72.48	2.663	135.51
	2.658	69.78	2.657	131.87
	<b>2.644</b>	<b>70.88</b>	<b>2.641</b>	<b>141.72</b>
MPWPBE	2.658	71.76	2.658	133.99
	2.652	69.34	2.650	130.08
	<b>2.639</b>	<b>70.26</b>	<b>2.635</b>	<b>141.54</b>
PBEPBE	2.664	71.58	2.663	133.86
	2.656	69.27	2.654	129.40
	<b>2.644</b>	<b>70.16</b>	<b>2.640</b>	<b>141.06</b>

<sup>a</sup>LanL2DZ plain. CEP-121 italic. SDD bold. MP2: LanL2DZ R = 2.750, angle = 68.29; CEP-121 R = 2.678, angle = 67.20; SDD R = **2.668**, angle = **67.31**. CCSD: LanL2DZ R = 2.778, angle = 69.09; CEP-121 R = 2.701, angle = 68.38; SDD R = **2.691**, angle = **68.28**. CCSD(T): LanL2DZ R = 2.775, angle = 68.53; CEP-121 R = 2.693, angle = 67.44; SDD R = **2.684**, angle = **67.57**.

other ECPs and their corresponding valence basis sets (see Tables 2 and 3) when the same density functional is used. Consequently, all of these results suggest that the geometry of the  $\text{Cu}_3$  and  $\text{Ag}_3$  obtained with GGA type functionals, depends not only on the correlation functional but also on the pseudopotential and the valence basis set. In conclusion, the GGA type density functionals do not seem to be very reliable for calculation of transition metal trimers of the 1b group.

Tables 4 and 5 show that, for H-GGA methods in general with CEP-121 and SDD ECP/valence basis set, the calculations with LYP correlation functional predict two structures regardless of the Hartree–Fock exchange percentage is in the functional. Only PBE1PBE and MPW1K agree with the CCSD, CCSD(T), and MP2 results for  $\text{Cu}_3$  and  $\text{Ag}_3$ , independently of the pseudopotential employed. It is noteworthy that CCSD as well as CCSD(T) and MP2 methods predict one minimum only, with all ECPs/valence basis sets. For  $\text{Au}_3$  cluster all functionals predict correctly two structures except for calculations done with B3LYP/LanL2dz, O3LYP/LanL2DZ, and O3LYP/SDD where only a single minimum near  $140^\circ$  was found. The seven tested HM-GGA functionals (see Supporting Information, Table S1) behave better than the GGA or H-GGA, for  $\text{Cu}_3$ . All functional predict correctly a single  $\text{Cu}_3$  minimum near  $\theta = 70$  in agreement with the ab initio post-

Table 4. Distances (in Å) and Bond Angles (in Degrees) for  $\text{Cu}_3$  ( $C_{2v}$ ) Clusters.  $^2B_2$  State Using Some H-GGA Functional<sup>a</sup>

functional	weight factor	R (Å)	angle (deg)	R (Å)	angle (deg)
O3LYP	0.1161	2.364	73.58	<b>2.344</b>	<b>116.75</b>
		2.357	69.89		
		<b>2.334</b>	<b>70.88</b>		
B3LYP	0.200	2.327	73.94	2.339	113.62
		2.340	70.04		
		<b>2.308</b>	<b>71.30</b>		
B3PW91	0.200	2.325	70.63	<b>2.310</b>	<b>117.10</b>
		2.326	68.43		
		<b>2.300</b>	<b>68.91</b>		
B3P86	0.200	2.312	70.43		
		2.315	68.34		
		<b>2.288</b>	<b>68.78</b>		
B97-1	0.210	2.342	74.85		
		2.347	70.54		
		<b>2.319</b>	<b>72.07</b>		
MPW3LYP	0.218	2.326	73.95	2.336	110.01
		2.338	70.03		
		<b>2.307</b>	<b>71.18</b>		
X3LYP	0.218	2.327	73.93	2.337	110.81
		2.339	70.04		
		<b>2.308</b>	<b>71.24</b>		
PBE1PBE	0.250	2.334	70.40		
		2.331	68.35		
		<b>2.306</b>	<b>68.73</b>		
MPW1K	0.428	2.347	71.91		
		2.342	69.51		
		<b>2.313</b>	<b>69.77</b>		
BH&HLYP	0.500	2.360	78.72		
		2.365	72.79		
		<b>2.330</b>	<b>74.48</b>		

<sup>a</sup>LanL2DZ plain. CEP-121 italic. SDD bold.

Hartree–Fock results. Regarding  $\text{Ag}_3$  (Supporting Information, Table S2), the results are not as good as in the  $\text{Cu}_3$  case. Only the BB1K and MPWB1K functionals predict correctly a single  $\text{Ag}_3$  minimum with all ECPs/valence basis sets used. The MPW1KCIS, PBE1KCIS, and BMK functionals predict two minima, one with an acute bond angle and other with an obtuse bond angle. It is worth noticing that, even though the BMK functional has the same Hartree–Fock exchange percentage that the BB1K functional, the results are completely different. On the other hand the B1BB5 and MPW1B95 functionals work well with LanL2DZ and CEP-121 pseudopotentials but no with SDD where two minimum energy structures appear.

Regarding the  $\text{Au}_3$  clusters in general, all HM-GGA functionals predict two structures with LanL2DZ and CEP-121 ECP/valence basis set in agreement with the CCSD/SDD calculations (see Table S3). On the contrary, in the case of the HM-GGA/SDD: B1B95, MPW1B95, BB1K, and MPWB1K, even though two stationary points were found with acute and obtuse bond angles, the structures with the obtuse bond angle have imaginary frequencies and therefore are not real minimum energy structures.

To analyze the influence of the HF-exchange percentage in the H-GGA functional, we performed a series of calculation changing the HF-exchange weight factor in a given functional and keeping the correlation part constant. Considering that the exchange-correlation energy  $E^{\text{xc}}$  can be written as:

Table 5. Distances (in Å) and Bond Angles (in Degrees) for  $\text{Ag}_3$  ( $C_{2v}$ ) Clusters.  $^2B_2$  State Using Some H-GGA Functional<sup>a</sup>

functional	weight factor	R (Å)	angle (deg)	R (Å)	angle (deg)
O3LYP	0.1161			2.732	149.70
				2.715	142.15
				<b>2.701</b>	<b>179.99</b>
B3LYP	0.200	2.683	75.92	2.694	141.83
				2.688	135.62
				<b>2.673</b>	<b>153.04</b>
B3PW91	0.200	2.668	73.19	2.669	126.80
		2.661	70.32	2.660	118.65
		<b>2.645</b>	<b>71.24</b>	<b>2.646</b>	<b>133.62</b>
B3P86	0.200	2.654	72.13	2.653	128.90
		2.649	67.76	2.645	119.43
		<b>2.634</b>	<b>70.59</b>	<b>2.631</b>	<b>134.14</b>
B97-1	0.210	2.669	78.32	2.696	142.48
		2.682	75.37	2.688	135.89
		<b>2.669</b>	<b>78.32</b>	<b>2.674</b>	<b>153.70</b>
MPW3LYP	0.218	2.680	74.57	2.692	140.82
				2.685	134.14
				<b>2.670</b>	<b>154.61</b>
X3LYP	0.218	2.681	74.84	2.693	140.98
				2.686	134.44
				<b>2.671</b>	<b>152.95</b>
PBE1PBE	0.250	2.670	72.13		
		2.661	69.72		
		<b>2.648</b>	<b>70.38</b>		
MPW1K	0.428	2.676	72.61		
		2.664	70.04		
		<b>2.652</b>	<b>70.61</b>		
BH&HLYP	0.500	2.697	75.57	2.714	133.11
				2.704	121.51
		<b>2.682</b>	<b>78.21</b>	<b>2.690</b>	<b>137.05</b>

<sup>a</sup>LanL2DZ plain. CEP-121 italic. SDD bold.

$$E^{\text{xc}} = \alpha E_{\text{HF}}^{\text{x}} + (1 - \alpha) E_{\text{DFT}}^{\text{x}} + E_{\text{DFT}}^{\text{c}} \quad (1)$$

where  $\alpha$  is the Hartree–Fock exchange weight factor,  $E_{\text{HF}}^{\text{x}}$  the HF-exchange energy, and  $E_{\text{DFT}}^{\text{x}}$  and  $E_{\text{DFT}}^{\text{c}}$  are the exchange and correlation density functionals, respectively. The  $\alpha$  value can be changed systematically without changing the correlation functional  $E_{\text{DFT}}^{\text{c}}$ .<sup>21</sup> We chose the MPW1K functional because this functional has a high  $\alpha$  value ( $\alpha = 0.428$ ) and the calculations with the three ECPs/valence basis sets predict correctly only one structure. In eq 1 when the  $\alpha$  value is 0.250, the  $E^{\text{xc}}$  corresponds to MPW1PW91 functional, while when  $\alpha = 0.428$ ,  $E^{\text{xc}}$  corresponds to MPW1K. Figure 2 displays the potential energy curves using the MPW1K functional with  $\alpha = 0.26$ , 0.27, and 0.28, and the SSD ECP/valence basis set for  $\text{Ag}_3$ . The minimum in the potential curves around 120–125° disappears as the  $\alpha$  value increases from 0.26 to 0.28 which shows the importance of  $\alpha$  in the stabilization/destabilization of certain structures. Table 6 shows that the effect of the  $\alpha$  value on the predicted structure with the acute angle ( $\sim 71^\circ$ ) is not as dramatic as the effect on the second structure where increasing slightly the  $\alpha$  value from 0.250 to 0.270, the bond angle changes from 126° to 118°; furthermore, in the range of 0.280–0.428, this last structure completely disappears, and the calculations predict that there is only one structure with an acute angle. From now in the text, the structures that show instabilities with small changes in  $\alpha$  will be called spurious structures. These

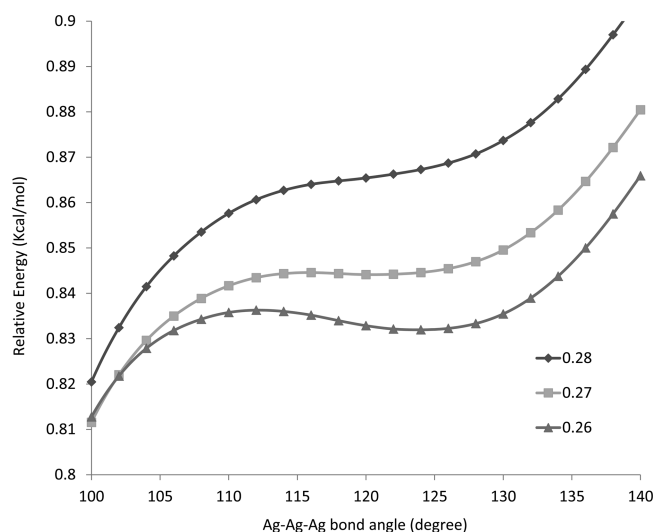


**Figure 2.** Detail of the potential energy curves for  $\text{Ag}_3$  as a function of the Ag–Ag–Ag angle using eq 1 and  $\alpha$  values of 0.26, 0.27, and 0.28. MPW1K( $\alpha$ )/SDD.

**Table 6.** HF Weight Factor, Distances (in Å), and Bond Angles (in Degrees) for  $\text{Ag}_3$  ( $C_{2v}$ )  $^2B_2$  H-GGA Functional/SDD

weight factor	$R$ (Å)	angle (deg)	$R$ (Å)	angle (deg)	$\Delta E$ kcal/mol
0.250 <sup>a</sup>	2.646	70.69	2.645	126.53	0.80
0.260	2.647	70.69	2.645	123.91	0.84
0.270	2.647	70.69	2.645	118.41	0.87
0.280	2.647	70.69			
0.300	2.648	70.68			
0.428 <sup>b</sup>	2.652	70.61			

<sup>a</sup>MPW1PW91 functional. <sup>b</sup>MPW1K functional.

results show that there is a compensation of errors between the Hartree–Fock exchange percentage in the functional and the exchange–correlation functional that can be manipulated partially changing the  $\alpha$  value. As stated by Yang, Cohen, and Mori-Sanchez in their review on DFT methods<sup>2</sup> “B3LYP is successful as a result of some cancellation of errors”. The density functionals are successful due to the appropriate cancellation of errors.<sup>1,2,6,42</sup>

As in the case of the diatomic molecules, the MUE and AMUE values were calculated. Because there is not experimental data available, we used the CCSD(T) method as the reference method for the geometrical parameter values. In general, for GGA, H-GGA, and HM-GGA methods, the bond length AMUE values are all equal to 0.04 Å. Regarding to the bond angles, the following AMUE values were obtained: GGA 2.6°, H-GGA 5.1°, and HM-GGA 3.2°. The maximum MUEs for the GGA, H-GGA, and HM-GGA methods corresponding to the bond length and bond angle were obtained with the LanL2DZ ECP/valence basis set. GGA-(LanL2DZ): bond length (MUE = 0.09 Å), bond angle (MUE = 2.35); H-GGA(LanL2DZ): bond length (MUE = 0.09 Å), bond angle (MUE = 6.13); HM-GGA(LanL2DZ): bond length (MUE = 0.08 Å), bond angle (MUE = 3.73).

**C. Anionic Tetramers:  $\text{Cu}_4^-$ ,  $\text{Ag}_4^-$ .** In this section, the results for  $\text{Cu}_4^-$  and  $\text{Ag}_4^-$  using the H-GGA and HM-GGA type functionals are presented. Four geometry types are possible for  $\text{M}_4^-$   $\text{M} = \text{Cu}, \text{Ag}$  clusters:  $D_{2h}$ ,  $C_{2v}$ ,  $C_{2h}$ , and  $D_{\infty h}$ , as shown in Figure 3. At MP2 and CCSD level, the

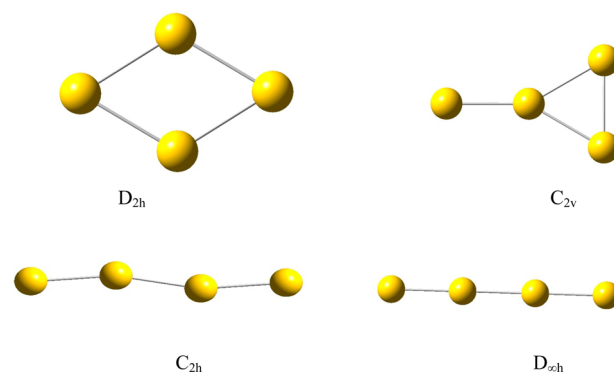


**Figure 3.**  $\text{M}_4^-$  structures,  $\text{M} = \text{Cu}, \text{Ag}$ .

relative energy of the  $\text{Cu}_4^-$  clusters follows the order:  $D_{2h} < C_{2v} < D_{\infty h}$ , as shown at the footnote in Table 7. No  $C_{2h}$  type structures were found at MP2 or CCSD level of theory. In general for  $\text{Cu}_4^-$  clusters (see Table 7), the H-GGA functionals reproduce qualitatively the MP2 and CCSD trend. On the other hand; calculations with CEP-121 and LanL2DZ and functionals with  $\alpha$  values lower or equal to 0.218 predict the  $C_{2h}$  structure as the real minimum and the linear structure  $D_{\infty h}$  with two imaginary frequencies. It is worth noticing that there is a change in the order of stability of the  $D_{\infty h}$  and  $C_{2v}$  structures when O3LYP/SDD and BH&HLYP/SDD are used, which is in disagreement with the MP2/SDD and CCSD/SDD results. These two functionals have the lower and higher values of the Hartree–Fock exchange factor, 0.1161 and 0.500, respectively. Noteworthy, unlike calculations with SDD, BH&HLYP calculations with LanL2DZ and CEP-121 predict the right energy order; i.e.,  $D_{2h} < C_{2v} < D_{\infty h}$ . This result suggests that the cancellation of errors in the functionals is affected by the ECP/valence basis set employed.

Table 8 shows that, for  $\text{Ag}_4^-$  clusters, only the PBE1PBE and MPW1K functionals reproduce the ab initio post-Hartree–Fock relative energy order with all ECP/valence basis sets. On the other hand, all functionals with Lee–Yang–Parr correlation functional predict wrongly the linear structure  $D_{\infty h}$  as the ground state structure.

Tables 9 and 10 show that the behavior of the HM-GGA functionals is better than the H-GGAs, except the functionals with low  $\alpha$  values such as MPW1KCIS and PBE1KCIS. To see the influence of the  $\alpha$  factor on the results obtained with HM-GGA functionals, we change the  $\alpha$  value of the MPW1B95( $\alpha = 0.31$ ) functional. This functional with SDD ECP/valence basis set fails in the case of  $\text{Ag}_3$  (see Table S2) predicting two stable structures, one with a bond angle of 69.2° and other one with a bond angle of 130.3°. Changing the  $\alpha$  value from 0.310 to 0.330, the false minimum at 130.3° obtained with MPW1B95/SDD disappears. The relative energy order for  $\text{Ag}_4^-$  clusters obtained using MPW1B95( $\alpha = 0.33$ )/SDD and MPW1B95( $\alpha = 0.33$ )/CEP-121 was:  $D_{2h}(E_{\text{rel.}} = 0.00 \text{ kcal/mol}) < C_{2v}(E_{\text{rel.}} = 2.99 \text{ kcal/mol}) < D_{\infty h}(E_{\text{rel.}} = 3.96 \text{ kcal/mol})$  and  $D_{2h}(E_{\text{rel.}} = 0.00 \text{ kcal/mol}) < C_{2v}(E_{\text{rel.}} = 3.8 \text{ kcal/mol}) < D_{\infty h}(E_{\text{rel.}} = 5.41 \text{ kcal/mol})$ , respectively. Comparing these results with those reported in Table 10 it is clear that there is not a significant change in the relative energy values. Therefore, one can conclude that the effect of  $\alpha$  on the relative energies of true minimums is lower than the corresponding effect on the spurious structures.

**D.  $[\text{H}_2\text{O}-\text{Cu}]^{+2}$  Case.** Sodupe et al.<sup>9</sup> analyzed the ground and low-lying states of the  $[\text{H}_2\text{O}-\text{Cu}]^{+2}$  complex. Using two

Table 7. Relative Energies in kcal/mol for  $\text{Cu}_4^-$  Clusters. H-GGA Type Functional<sup>a</sup>

functional	HF weight factor	$D_{2h}$ ( $^2B_{2u}$ )	$C_{2v}$ ( $^2B_2$ )	$C_{2h}$ ( $^2A_g$ )	$D_{\infty h}$ ( $^2\Sigma_g^+$ )
O3LYP	0.1161	0.00	3.88	6.05, $\theta = 172.21$	6.05 <sup>b</sup>
		0.00	3.60	5.47, $\theta = 174.03$	5.47 <sup>b</sup>
		<b>0.00</b>	<b>4.46</b>		<b>2.93</b>
B3LYP	0.200	0.00	3.70	5.33, $\theta = 176.25$	5.86
		0.00	3.48		5.33 <sup>b</sup>
		<b>0.00</b>	<b>2.40</b>		<b>3.04</b>
B3PW91	0.200	0.00	5.50	9.71, $\theta = 174.76$	9.72 <sup>b</sup>
		0.00	5.28	9.16, $\theta = 176.58$	9.16 <sup>b</sup>
		<b>0.00</b>	<b>4.39</b>		<b>7.25</b>
B3P86	0.200	0.00	5.81	9.65, $\theta = 177.60$	9.96
		0.00	5.67		9.65 <sup>b</sup>
		<b>0.00</b>	<b>4.75</b>		<b>7.70</b>
B97-1	0.210	0.00	5.58	6.94, $\theta = 177.42$	7.72
		0.00	5.17		6.94 <sup>b</sup>
		<b>0.00</b>	<b>4.08</b>		<b>4.70</b>
MPW3LYP	0.218	0.00	3.89	5.71, $\theta = 177.31$	6.17
		0.00	3.72		5.72 <sup>b</sup>
		<b>0.00</b>	<b>2.63</b>		<b>3.46</b>
X3LYP	0.218	0.00	3.80	5.53, $\theta = 177.41$	6.02
		0.00	3.61		5.53 <sup>b</sup>
		<b>0.00</b>	<b>2.54</b>		<b>3.29</b>
PBE1PBE	0.250	0.00	6.10		10.78
		0.00	5.91		10.18
		<b>0.00</b>	<b>5.09</b>		<b>8.45</b>
MPW1K	0.428	0.00	8.08		7.83
		0.00	4.60		7.30
		<b>0.00</b>	<b>4.10</b>		<b>6.36</b>
BH&HLYP	0.500	0.00	2.10		2.62
		0.00	2.02		2.07
		<b>0.00</b>	<b>1.40</b>		<b>0.88</b>

<sup>a</sup>LanL2DZ plain. CEP-121 italic. **SDD bold**. MP2/LanL2DZ relative energy:  $D_{2h}$  (0.00) <  $C_{2v}$  (+9.2 kcal/mol) <  $D_{\infty h}$  (+13.6 kcal/mol); MP2/CEP-121 relative energy:  $D_{2h}$  (0.00) <  $C_{2v}$  (+13.5 kcal/mol) <  $D_{\infty h}$  (+19.2 kcal/mol); MP2/SDD relative energy:  $D_{2h}$  (0.00) <  $C_{2v}$  (+11.7 kcal/mol) <  $D_{\infty h}$  (+17.2 kcal/mol); CCSD/LanL2DZ relative energy:  $D_{2h}$  (0.00) <  $C_{2v}$  (+3.9 kcal/mol) <  $D_{\infty h}$  (+5.6 kcal/mol); CCSD(T)/LanL2DZ relative energy:  $D_{2h}$  (0.00) <  $C_{2v}$  (+5.1 kcal/mol) <  $D_{\infty h}$  (+9.3 kcal/mol); CCSD/SDD relative energy:  $D_{2h}$  (0.00 kcal/mol) <  $C_{2v}$  (+3.5 kcal/mol) <  $D_{\infty h}$  (+5.1 kcal/mol). <sup>b</sup>Two imaginary frequencies.

GGA type and three H-GGA type functionals they concluded that the relative stability of the electronic states,  $^2A_1 < ^2B_1 < ^2B_2 < ^2A_2$ , depends on the degree of mixing of exact HF and DFT exchange functional. For GGA and H-GGA with  $\alpha$  lower or equal to 0.25, the  $^2B_1$  state is more stable than the  $^2A_1$  one. Moreover, with these functionals the structure with  $C_s$  geometry is the groundstate; at the CCSD(T) level this structure does not exist. We reanalyzed the  $[\text{H}_2\text{O}-\text{Cu}]^{+2}$  case and found that in general, with GGA type functionals, the  $^2A'$  state ( $C_s$  symmetry) is the ground state in agreement with Sodupe's results. On the other hand the  $^2B_1$  state, which is lower in energy than the  $^2A_1$ , has one imaginary frequency and corresponds to a transition state between two  $C_s$  symmetry structures. The performance of the H-GGA and HM-GGA type functionals are better than the GGA; however, it is necessary to reach at least one  $\alpha$  value of 0.420 (see Tables S5 and S6) to obtain the same CCSD(T) relative stability order without the

Table 8. Relative Energies in kcal/mol for  $\text{Ag}_4^-$  Clusters. H-GGA Type Functionals<sup>a</sup>

functional	HF weight factor	$D_{2h}$ ( $^2B_{2u}$ )	$C_{2v}$ ( $^2B_2$ )	$D_{\infty h}$ ( $^2\Sigma_g^+$ )
O3LYP	0.1161	4.75	3.60	0.00
		5.43	3.78	0.00
		<b>3.27</b>	<b>2.67</b>	<b>0.00</b>
B3LYP	0.200	2.30	2.10	0.00
		2.93	2.48	0.00
		<b>0.82</b>	<b>1.46</b>	<b>0.00</b>
B3PW91	0.200	0.00	1.12	0.60
		0.00	1.03	0.37
		<b>0.00</b>	<b>2.22</b>	<b>2.00</b>
B3P86	0.200	0.00	1.62	1.29
		0.00	1.52	1.01
		<b>0.00</b>	<b>2.56</b>	<b>3.00</b>
B97-1	0.210	0.91	2.24	0.00
		1.47	2.49	0.00
		<b>0.58</b>	<b>1.62</b>	<b>0.00</b>
MPW3LYP	0.218	1.70	1.83	0.00
		2.47	2.30	0.00
		<b>2.30</b>	<b>2.28</b>	<b>0.00</b>
X3LYP	0.218	1.90	1.90	0.00
		2.51	2.27	0.00
		<b>2.50</b>	<b>2.27</b>	<b>0.00</b>
PBE1PBE	0.250	0.00	1.87	2.05
		0.00	1.81	1.89
		<b>0.00</b>	<b>2.77</b>	<b>3.64</b>
MPW1K	0.428	0.00	1.21	1.25
		0.00	2.05	2.70
		<b>0.00</b>	<b>1.39</b>	<b>1.51</b>
BH&HLYP	0.500	2.41	1.76	0.00
		1.32	1.36	0.00
		<b>2.61</b>	<b>1.94</b>	<b>0.00</b>

<sup>a</sup>LanL2DZ plain. CEP-121 italic. **SDD bold**. MP2/LanL2DZ relative energy:  $D_{2h}$  (0.00 kcal/mol) <  $C_{2v}$  (+7.2 kcal/mol) <  $D_{\infty h}$  (+9.0 kcal/mol); MP2/CEP-121 relative energy:  $D_{2h}$  (0.00 kcal/mol) <  $C_{2v}$  (+9.4 kcal/mol) <  $D_{\infty h}$  (+11.7 kcal/mol); **MP2/SDD relative energy**:  $D_{2h}$  (0.00 kcal/mol) <  $C_{2v}$  (+8.5 kcal/mol) <  $D_{\infty h}$  (+11.9 kcal/mol); CCSD/LanL2DZ relative energy:  $D_{2h}$  (0.00 kcal/mol) <  $C_{2v}$  (+1.7 kcal/mol) <  $D_{\infty h}$  (+2.4 kcal/mol); CCSD(T)/LanL2DZ relative energy:  $D_{2h}$  (0.00 kcal/mol) <  $C_{2v}$  (+2.9 kcal/mol) <  $D_{\infty h}$  (+4.3 kcal/mol); **CCSD/SDD relative energy**:  $D_{2h}$  (0.00 kcal/mol) <  $C_{2v}$  (+1.9 kcal/mol) <  $D_{\infty h}$  (+3.2 kcal/mol).

spurious  $C_s$  symmetry structures. This result point out that, for  $[\text{H}_2\text{O}-\text{Cu}]^{+2}$  case, it is more important to have a high HF exchange percentage than the exchange-correlation type functional in the density functionals.

## CONCLUSIONS

Results for  $M_3$  and  $M_4^-$ ,  $M = \text{Cu}, \text{Ag}, \text{Au}$ , clusters seem to point out that it is necessary to develop more confident functionals. GGA type functionals, in general, failed in all studied cases. The inclusion of the Hartree-Fock exchange in the functional (H-GGA) seems to have improved results; however, the results with these H-GGA types functional show dependence with the ECP/valence basis set used; i.e., some false minima can appear with some ECP/valence basis sets, inducing wrong conclusions on the existence of isomers. This type of dependence was not found in MP2, CCSD or CCSD(T) calculations. On the other hand, H-GGA functionals with LYP correlation functional fail in the description of  $M_3$  and  $M_4^-$  clusters,  $M = \text{Cu}, \text{Ag}$ . Some authors have proposed<sup>8,42</sup> that this fail is due to the fact that the



**Table 9. Relative Energies in kcal/mol for  $\text{Cu}_4^-$  Clusters. HM-GGA Type Functionals<sup>a</sup>**

functional	HF weight factor	$D_{2h}$ ( $^2B_{2u}$ )	$C_{2v}$ ( $^2B_2$ )	$C_{2h}$ ( $^2A_g$ )	$D_{\infty h}$ ( $^2\Sigma_g^+$ )
MPW1KCIS	0.150	0.00	5.35	9.24, $\theta = 169.35$	9.26 <sup>b</sup>
		0.00	4.99	8.42, $\theta = 173.00$	8.43 <sup>b</sup>
		<b>0.00</b>	<b>3.97</b>		<b>6.25</b>
PBE1KCIS	0.220	0.00	5.23		8.82
		0.00	4.86		7.87
		<b>0.00</b>	<b>3.97</b>		<b>5.98</b>
B1B95	0.280	0.00	6.99		11.99
		0.00	6.58		10.85
		<b>0.00</b>	<b>6.08</b>		<b>9.74</b>
MPW1B95	0.310	0.00	7.07		12.04
		0.00	6.69		10.96
		<b>0.00</b>	<b>6.24</b>		<b>9.99</b>
BB1K	0.420	0.00	6.35		10.68
		0.00	6.00		9.52
		<b>0.00</b>	<b>5.77</b>		<b>9.06</b>
BMK	0.420	0.00	5.97		9.57
		0.00	4.98		6.57
		<b>0.00</b>	<b>4.78</b>		<b>6.35</b>
MPWB1K	0.440	0.00	6.46		10.81
		0.00	6.12		9.69
		<b>0.00</b>	<b>5.92</b>		<b>9.31</b>

<sup>a</sup>LanL2DZ plain. CEP-121 italic. SDD bold. <sup>b</sup>2 imaginary frequencies.**Table 10. Relative Energies in kcal/mol for  $\text{Ag}_4^-$  Clusters. HM-GGA Type Functionals<sup>a</sup>**

functional	HF weight factor	$D_{2h}$ ( $^2B_{2u}$ )	$C_{2v}$ ( $^2B_2$ )	$D_{\infty h}$ ( $^2\Sigma_g^+$ )
MPW1KCIS	0.150	0.54	1.28	0.00
		0.00	1.57	0.54
		<b>1.10</b>	<b>1.61</b>	<b>0.00</b>
PBE1KCIS	0.220	0.11	1.04	0.00
		0.00	1.75	1.30
		<b>0.62</b>	<b>1.36</b>	<b>0.00</b>
B1B95	0.280	0.00	2.67	3.42
		0.00	3.56	4.94
		<b>0.00</b>	<b>2.69</b>	<b>3.35</b>
MPW1B95	0.310	0.00	2.94	3.90
		0.00	3.83	5.42
		<b>0.00</b>	<b>2.99</b>	<b>3.91</b>
BB1K	0.420	0.00	2.57	3.55
		0.00	3.45	4.97
		<b>0.00</b>	<b>2.76</b>	<b>3.79</b>
BMK	0.420	0.00	1.71	1.65
		0.00	2.71	3.14
		<b>0.00</b>	<b>1.37</b>	<b>0.65</b>
MPWB1K	0.440	0.00	2.80	3.94
		0.00	3.67	5.35
		<b>0.00</b>	<b>3.00</b>	<b>4.22</b>

<sup>a</sup>LanL2DZ plain. CEP-121 italic. SDD bold.

LYP correlation functional does not satisfy the correct electron gas limit<sup>8</sup> and underestimate the correlation energy of the homogeneous electron gas;<sup>42</sup> therefore, it is important to work with correlation functionals that satisfy the electron gas limit such as PW91, PBE, B95, and so forth, to obtain the correct results. Even though our results support this conclusion, it is clear that it is necessary but not sufficient to satisfy the electron gas limit. Density functionals with B95 correlation functional

such as B1B95 or MPW1B95 and functionals with PW91 such as MPW1PW91 fail in the calculation of the  $\text{Ag}_3$  cluster (Tables 6 and S2).

Our results point out that the HF-exchange percentage in the H-GGA functionals helps to improve the results, compensating in some way the functional errors. Changing slightly the  $\alpha$  value, some minima in the energy potential surface can completely disappear. These minimums or spurious structures do not appear when ab initio correlated methods such as MP2, CCSD, or CCSD(T) are used. The existence of the spurious structures is an indication of the delicate balance in the compensation of errors in the functionals. On the other hand, there is not a straightforward correlation between the  $\alpha$  values, and the final results, for example, the relative energy order for  $\text{Cu}_4^-$  calculated with O3LYP( $\alpha = 0.1161$ )/SDD or BH&HLYP( $\alpha = 0.500$ )/SDD is in disagreement with the MP2/SDD or CCSD/SDD results but the MPW3LYP( $\alpha = 0.218$ )/SDD and X3LYP( $\alpha = 0.218$ )/SDD, reproduce the relative energy order given by the post Hartree–Fock methods. The HM-GGA type functionals seem to behave better than the H-GGA type functionals, been the BB1K( $\alpha = 0.420$ ) and MPWB1K( $\alpha = 0.440$ ) functionals with all ECP/valence basis sets those that reproduce in almost all cases studied herein, the MP2, CCSD, and CCSD(T) results. These two functionals have in common that have the B95 correlation functional. Others functional with the B95 correlation functional but with low  $\alpha$  values such as MPW1B95( $\alpha = 0.310$ ) fail in the calculation of  $\text{Ag}_3$  structures with SDD showing once more, the delicate compensation of errors between the Hartree–Fock exchange percentage and the exchange-correlation functional. In spite of the fact that more theoretical studies are necessary to improve the functional, the BB1K and MPWB1K functionals seem to be the logical choice at the moment to calculate small metallic clusters. One possible strategy to check if the structures are spurious or not, is to perform calculations increasing slightly the  $\alpha$  value in the functional, if the structure disappears or drastic change are observed in its geometrical parameters, it was a false minimum. Regarding the  $[\text{H}_2\text{O}-\text{Cu}]^{+2}$  case, our and the Sodupe et al.<sup>9</sup> results show that it is more important the Hartree–Fock exchange percentage than the type of exchange or correlation functional and at least one  $\alpha$  value of 0.400 in the functional to reproduce the electronic state and relative energy order given by high correlated ab initio methods such as CCSD(T).

## ■ ASSOCIATED CONTENT

### § Supporting Information

Distances and bond angles for  $\text{Cu}_3$  ( $C_{2v}$ ) clusters using HM-GGA type functional (Table S1), distances and bond angles for  $\text{Ag}_3$  ( $C_{2v}$ ) clusters using HM-GGA type functional (Table S2), distances and bond angles for  $\text{Au}_3$  ( $C_{2v}$ ) clusters using HM-GGA type functional (Table S3), relative energies between the first electronic states of  $[\text{H}_2\text{O}-\text{Cu}]^{+2}$  complex using GGA type functional (Table S4), relative energies between the first electronic states of  $[\text{H}_2\text{O}-\text{Cu}]^{+2}$  using H-GGA type functional (Table S5), and relative energies between the first electronic states of  $[\text{H}_2\text{O}-\text{Cu}]^{+2}$  complex using HM-GGA type functional (Table S6). This material is available free of charge via the Internet at <http://pubs.acs.org>.

## ■ AUTHOR INFORMATION

### Notes

The authors declare no competing financial interest.

## REFERENCES

- (1) Sousa, S. F.; Fernandes, P. A.; Ramos, M. J. General Performance of Density Functionals. *J. Phys. Chem. A* **2007**, *111*, 10439–10452.
- (2) Cohen, A. J.; Mori-Sanchez, P.; Yang, W. Challenges for Density Functional Theory. *Chem. Rev.* **2012**, *112*, 289–320.
- (3) Cramer, C. J.; Truhlar, D. G. Density functional theory for transition metals and transition metal chemistry. *Phys. Chem. Chem. Phys.* **2009**, *11*, 10757–10816.
- (4) Strassner, T.; Taige, M. A. Evaluation of Functionals O3LYP, KMLYP, and MPW1K in Comparison to B3LYP for Selected Transition-Metal Compounds. *J. Chem. Theory Comput.* **2005**, *1*, 848–855.
- (5) Barden, C. J.; Rienstra-Kiracofe, J. C.; Schaefer, H. F., III. Homonuclear 3d transition-metal diatomics: A systematic density functional theory study. *J. Chem. Phys.* **2000**, *113*, 690–700.
- (6) Ramírez-Solís, A. On the performance of local, semilocal, and nonlocal exchange-correlation functionals on transition metal molecules. *J. Chem. Phys.* **2007**, *126*, 224105.
- (7) Yang, X.-F.; Wang, Y.-L.; Zhao, Y.-F.; Wang, A.-Q.; Zhang, T.; Li, J. Adsorption-induced structural changes of gold cations from two- to three-dimensions. *Phys. Chem. Chem. Phys.* **2010**, *12*, 3038–3043.
- (8) Zhao, S.; Li, Z.-H.; Wang, W. N.; Liu, Z.-P.; Fan, K.-N.; Xie, Y.; Schaefer, H. F., III. Is the uniform electron gas limit important for small Ag clusters? Assessment of different density functionals for  $\text{Ag}_n$  ( $n \leq 4$ ). *J. Chem. Phys.* **2006**, *124*, 184102.
- (9) Sola, J. P. M.; Rimola, A.; Rodriguez-Santiago, L.; Sodupe, M. Ground and Low-Lying States of  $\text{Cu}^+-\text{H}_2\text{O}$ . A Difficult Case for Density Functional Methods. *J. Phys. Chem. A* **2004**, *108*, 6072–6078.
- (10) Schwerdtfeger, P.; Lein, M.; Krawczyk, R. P.; Jacob, C. R. The adsorption of CO on charged and neutral Au and Au<sub>2</sub>: A comparison between wave-function based and density functional theory. *J. Chem. Phys.* **2008**, *128*, 124302.
- (11) Gaussian 03, Revision D.02; Frisch, M. J.; Trucks, G. W.; Schlegel, H. B.; Scuseria, G. E.; Robb, M. A.; Cheeseman, J. R.; Montgomery, J. A.; Vreven, T., Jr.; Kudin, K. N.; Burant, J. C., et al. Gaussian, Inc.: Wallingford, CT, 2004.
- (12) Reiher, M.; Salomon, O.; Hess, B. A. Reparametrization of hybrid functionals based on energy differences of states of different multiplicity. *Theor. Chem. Acc.* **2001**, *107*, 48–55.
- (13) Bartlett, R. J. Many-body perturbation theory and coupled cluster theory for electron correlation in molecules. *Annu. Rev. Phys. Chem.* **1981**, *32*, 359–401.
- (14) Hay, P. J.; Wadt, W. R. Ab initio effective core potentials for molecular calculations. Potentials for K to Au including the outermost core orbitals. *J. Chem. Phys.* **1985**, *1*, 299–310.
- (15) Stevens, W. J.; Krauss, M.; Bash, H.; Jasien, P. G. Relativistic compact effective potentials and efficient, shared-exponent basis sets for the third-, fourth-, and fifth-row atoms. *Can. J. Chem.* **1992**, *70*, 612–630.
- (16) Andrae, D.; Häußermann, U.; Dolg, M.; Stoll, H.; Preuß, H. Energy-adjusted ab initio pseudopotentials for the second and third row transition elements. *Theor. Chim. Acta* **1990**, *77*, 123–141.
- (17) Hill, J. G.; Peterson, K. A. Explicitly Correlated Coupled Cluster Calculations for Molecules Containing Group 11 (Cu, Ag, Au) and 12 (Zn, Cd, Hg) Elements: Optimized Complementary Auxiliary Basis Sets for Valence and Core–Valence Basis Sets. *J. Chem. Theory Comput.* **2012**, *8*, 518–526.
- (18) Schultz, N. E.; Zhao, Y.; Truhlar, D. G. Databases for Transition Element Bonding: Metal-Metal Bond Energies and Bond Lengths and Their Use To Test Hybrid, Hybrid Meta, and Meta Density Functionals and Generalized Gradient Approximations. *J. Phys. Chem. A* **2005**, *109*, 4388–4403.
- (19) Weigend, F.; Ahlrichs, R. Balanced basis sets of split valence, triple zeta valence and quadruple zeta valence quality for H to Rn: Design and assessment of accuracy. *Phys. Chem. Chem. Phys.* **2005**, *7*, 3297–3305.
- (20) Feller, D. The role of databases in support of computational chemistry calculations. *J. Comput. Chem.* **1996**, *17*, 1571–1586.
- Schuchardt, K. L.; Didier, B. T.; Elsethagen, T.; Sun, L.; Gurumoorhi, V.; Chase, J.; Li, J.; Windus, T. L. Basis Set Exchange: A Community Database for Computational Sciences. *J. Chem. Inf. Model.* **2007**, *47*, 1045–1052; EMSL library.
- (21) We have made use of the G03 program feature that allows one to vary the functionals standard parameter set through internal options. To do this, one must define the Gaussian route as # MPWPW91 IOP(3/76 = P1P2). The new  $E^{\text{xc}}$  energy is therefore given by  $E^{\text{xc}} = p2E_{\text{HF}}^{\text{x}} + p1(E_{\text{LDA}}^{\text{x}} + E_{\text{MPW}}^{\text{x}}) + E_{\text{PW91}}^{\text{c}}$ , where  $pi = Pi/10000$ , for  $i = 1, 2$ . The MPW1K correspond to the set:  $p1 = 0.4280$  and  $p2 = 0.5720$ .
- (22) Becke, A. D. Density-functional exchange-energy approximation with correct asymptotic behavior. *Phys. Rev. A* **1988**, *38*, 3098–3100.
- (23) Lee, C.; Yang, W.; Parr, R. G. Development of the Colle-Salvetti correlation-energy formula into a functional of the electron density. *Phys. Rev. B* **1988**, *37*, 785–789.
- (24) Handy, N. C.; Cohen, A. J. Left-right correlation energy. *Mol. Phys.* **2001**, *99*, 403–412.
- (25) Adamo, C.; Barone, V. Exchange functionals with improved long-range behavior and adiabatic connection methods without adjustable parameters: The mPW and mPW1PW models. *J. Chem. Phys.* **1998**, *108*, 664–675.
- (26) Perdew, J. P. In *Electronic Structure of Solids*; Ziesche, P., Eischrig, H., Eds.; Akademie Verlag: Berlin, 1991; pp 11–22.
- (b) Perdew, J. P.; Wang, Y. Accurate and simple analytic representation of the electron-gas correlation energy. *Phys. Rev. B* **1992**, *45*, 13244–13249.
- (27) Perdew, J. P. Density-functional approximation for the correlation energy of the inhomogeneous electron gas. *Phys. Rev. B* **1986**, *33*, 8822–8824. (b) Perdew, J. P.; Wang, Y. Density-functional approximation for the correlation energy of the inhomogeneous electron gas. *Phys. Rev. B* **1986**, *33*, 8800–8802.
- (28) Perdew, J. P.; Burke, K.; Ernzerhof, M. Generalized Gradient Approximation Made Simple. *Phys. Rev. Lett.* **1996**, *77*, 3865–3868.
- (29) Hoe, W. M.; Cohen, A. J.; Handy, N. C. Assessment of a new local exchange functional OPTX. *Chem. Phys. Lett.* **2001**, *341*, 319–328.
- (30) Becke, A. D. Density–functional thermochemistry. III. The role of exact exchange. *J. Chem. Phys.* **1993**, *98*, 5648–5652.
- (31) Becke, A. D. Density–functional thermochemistry. IV. A new dynamical correlation functional and implications for exact–exchange mixing. *Phys. Rev. A* **1996**, *104*, 1040–1046.
- (32) Hamprecht, F. A.; Cohen, A. J.; Tozer, D. J.; Handy, N. C. Development and assessment of new exchange–correlation functionals. *J. Phys. Chem. A* **1998**, *109*, 6264–6271.
- (33) Perdew, J. P.; Wang, Y. Accurate and simple analytic representation of the electron-gas correlation energy. *Phys. Rev. B* **1992**, *45*, 13244–13249.
- (34) Lynch, B. J.; Fast, P. L.; Harris, M.; Truhlar, D. G. Adiabatic Connection for Kinetics. *J. Phys. Chem. A* **2000**, *104*, 4811–4815.
- (35) Lynch, B. J.; Zao, Y.; Truhlar, D. G. Effectiveness of Diffuse Basis Functions for Calculating Relative Energies by Density Functional Theory. *J. Phys. Chem. A* **2003**, *107*, 1384–1388.
- (36) (a) Krieger, J. B.; Chen, J.; Lafrate, G. J.; Savin, A. In *Electronic Correlation of Materials Prop.*; Gonis, A., Kioussis, N., Eds.; Plenum: New York, 1999; pp 463–477. (b) Kurth, S.; Perdew, J. P.; Blaha, P. Molecular and solid-state tests of density functional approximations: LSD, GGAs, and meta-GGAs. *Int. J. Quantum Chem.* **1999**, *75*, 889–909.
- (37) Zhao, Y.; Gonzalez-Garcia, N.; Truhlar, D. G. Benchmark Database of Barrier Heights for Heavy Atom Transfer, Nucleophilic Substitution, Association, and Unimolecular Reactions and Its Use to Test Theoretical Methods. *J. Phys. Chem. A* **2005**, *109*, 2012–2018.
- (38) Zhao, Y.; Truhlar, D. G. Benchmark Databases for Nonbonded Interactions and Their Use To Test Density Functional Theory. *J. Comput. Theory Comput.* **2005**, *1*, 415–432.
- (39) Zhao, Y.; Linch, B. J.; Truhlar, D. G. Development and Assessment of a New Hybrid Density Functional Model for Thermochemical Kinetics. *J. Phys. Chem. A* **2004**, *108*, 2715–2719.

- (40) Boese, A. D.; Martin, J. M. L. Development of density functionals for thermochemical kinetics. *J. Chem. Phys.* **2004**, *121*, 3405–3416.
- (41) Zhao, Y.; Truhlar, D. G. Hybrid Meta Density Functional Theory Methods for Thermochemistry, Thermochemical Kinetics, and Noncovalent Interactions: The MPW1B95 and MPWB1K Models and Comparative Assessments for Hydrogen Bonding and van der Waals Interactions. *J. Phys. Chem. A* **2004**, *108*, 6908–6918.
- (42) Paier, J.; Marsman, M.; Kresse, G. Why does the B3LYP hybrid functional fail for metals? *J. Chem. Phys.* **2007**, *127*, 024103.